MM Science Journal | www.mmscience.eu
ISSN 1803-1269 (Print) | ISSN 1805-0476 (On-line)
Special Issue | HSM 2025
18th International Conference on High Speed Machining
October 15-16, 2025, Metz, France
DOI: 10.17973/MMSJ.2025_12_2025165

HSM2025-44949

NEURAL NETWORKS FOR SIMULATED MICRO-FEATURE EVALUATION AND CLASSIFICATION

R. Bejjani[1*], C. AlLabaky[1]

[1]Lebanese American University, Department of Mechanical and Industrial Engineering, Byblos, Lebanon

*Corresponding author; e-mail: rolandbejj@gmail.com

Abstract
In recent years, advanced manufacturing has gained traction, particularly in the microscale industries, to enhance material properties. Creating micro-textures and achieving precise accuracy at the microscale are crucial for the performance of modern devices. In this paper, a method of facilitating these measures will be presented with the integration of Artificial Neural Networks (ANNs) to find the nonlinear relationship between the machining input parameters and the output microstructures' geometrical shapes. GoogleNet, a kind of Convolutional Neural Networks (CNNs), was also used to categorize the images between defective and ideal dimples to reach optimum precision in the manufacturing context.

Keywords:
Ultrasonic Vibration Assisted Turning; Artificial Neural Networks; GoogleNet

1 INTRODUCTION

In recent years, research has become more focused on micro-manufacturing to generate enhanced material properties that would result in remarkable improvements in surface quality. Miniaturization, which refers to the manufacturing of parts or features whose overall dimensions lie in the range of 1 to 500µm, is increasingly sought after in industries that require high precision. The following advancements are particularly critical in high-tech industries, including automotive, aerospace, and biological sectors. As these manufacturing processes evolve, there is a growing need for intelligent monitoring tools that leverage AI and image processing to enhance precision and efficiency. This paper presents a novel approach to micro-manufacturing by including the latter.

At the core of this innovation is Ultrasonic Vibration Assisted Turning (UVAT) in the radial direction. In this process, piezoelectric materials convert electrical energy to mechanical vibrations in the micro-scale, imprinting micro-textures and improving their material properties [Sharma 2016].

To bridge the gap between static manufacturing methods and the need for dynamic manufacturing solutions, advanced monitoring techniques and quality control methods should be employed [Heidari 2015]. For this reason, the development of intelligent machining and smart tools is revolutionizing manufacturing, leading to operations with higher accuracy, reduced costs, and more environmentally friendly processes. Central to this shift is the initiation of the "Smart Factory," which envisions fully automated manufacturing processes that integrate Internet-of-Things, Artificial Intelligence (AI), and big data with traditional manufacturing methods. The process will thus be as follows: generation, transmission, and processing of data to form a complete closed control system and minimize the need for human intervention [Osterrieder 2020].

A fundamental aspect of "Smart Factory" is the transition from primitive quality control methods like sampling, inspection, and benchmarking to modern AI-driven real-time analysis methodologies. To ensure better performance, increased production efficiency, and longevity of mechanical processes, the integration of AI is paramount. Through its various predictive analytics, real-time monitoring, and adaptive inference, AI provides the needed accuracy and adaptability to fill in the gaps that stem from traditional methods [Wang 2017].

This paper proposes a novel quality control approach that incorporates AI in the form of ANN and CNN. The ANN will be used to find the relationship between machining input parameters and micro-textures geometry with UVAT. As for CNN, it will categorize simulated features of different shapes to provide precise and adaptable solutions for manufacturing companies.

2 LITERATURE REVIEW

2.1 Ultrasonic Vibration Assisted Turning (UVAT)

"Vibro-impact cutting" was performed on optical slugs. The presence of these vibrations and the condition of the periodic separation that was studied had a positive impact on reducing the surface roughness as well as improving the working conditions [Lengerov 2023]. Similar studies across

the years have been using ultrasonic vibrations in turning operations to create microstructures that were deemed appropriate for lubrication and decreased friction. An experiment on the machining of an aluminum alloy (AA2017) was conducted using UVAT in cutting, feed, and radial directions. As a result, low-speed intermittent cutting had the following effects in each direction: rectangular micro-textures were formed in the cutting direction, dimples were formed in the radial direction, and sinusoidal ridges were formed in the feed direction, in which each has its own advantages. The average cutting force decreased with these vibrations, leading to the extension of tool life and a better surface finish [Schubert 2011]. Compressive residual stresses and the reduction of voids while using UVAT were also studied in the three previously mentioned directions. In the radial direction, there has been a significant reduction of voids, which leads to elevated compressive residual stresses [Nestler 2014].

Another study encompasses the experimentation on continuous turning of copper 1100 by using diamond tool inserts in the radial direction. The effects of altering the clearance angle and nose radius on the dimple profile were analyzed [Liu 2018].

While in some cases having larger circular micro-textures is considered more beneficial, Wang et al. preferred the elliptical smaller ones (created at lower spindle speeds) that resulted in a higher texture density where coating adhesion was enhanced. Therefore, the Si-P had a thicker coating, better wettability, less cracks, and higher bend strength [Wang 2022].

The importance of piezoelectric materials is further portrayed in previous literature. The piezoelectric actuator can reduce the error to up to 75% when compared to the first-stage actuator that generated an error of less than 10 microns [Krishnamoorthy 2004]. These actuators can be used for both low and high frequencies.

Kinematic relations were established between the cutting parameters and the dimple geometry based on their theoretical models without considering the complexity of elastoplastic deformations of each material.

Fig 1. shows the dimples' arrangement and geometry.

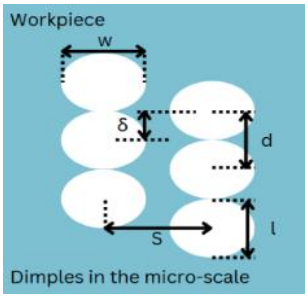

Fig. 1 Micro-Textures Geometry

The cutting speed can be expressed through the following equation:

$$V_c = \frac{\pi R n}{30} \quad (1)$$

Where "R" is the radius of the workpiece and "n" the spindle speed (rev/min).

The distance "d" between adjacent dimples is calculated by dividing the cutting speed by the ultrasonic frequency "f_{us}" in Hz. This distance which is equal to the length of a dimple is calculated as follows:

$$d = \frac{V_c}{f_{us}} = l \quad (2)$$

Finding the width "w" of the dimple is dependent on the nose radius "Rc" of the tool and the amplitude of vibrations "A," based on this equation:

$$w = 2\sqrt{R_c^2 - (R_c - 2A)^2} \quad (3)$$

Finally, to find the phase shift "δ" between the dimples, the cutting frequency ratio "λ" should be found:

$$\lambda = \frac{60\, f_{us}}{n} = K + \varepsilon \quad (4)$$

Where "K" is the number of dimples about one circumferential workpiece surface and "ε" is a fraction constant. This leads us to the phase shift equation that is equal to zero when the dimples are aligned [Liu 2019].

$$\delta = \frac{2\pi R \varepsilon}{\lambda} \quad (5)$$

2.2 ANN

The surface finish of a turned workpiece is affected by several factors that are unaccounted for in theoretical calculations, like unstable built-up edge (BUE), cutting fluids, machine tools, vibrations, thermally induced errors, etc. Hence, setting up an artificial neural network to compensate for these theoretical discrepancies was done.

The uses of various kinds of AI in modeling the complex relationships between the process parameters and the surface roughness of AISI 4140 steel were also explored. The performance of ANN, fuzzy logic, and multi-regression models from MATLAB were compared. ANN was able to achieve higher accuracy and more convergence with larger datasets [Akkus 2011].

The ANN architecture consists of the input layer, which receives its information from external sources and feeds it to the hidden layers. In this case, the input parameters are the cutting speed, feed rate, depth of cut, feed force, and cutting force. The hidden layer is responsible for processing the information and relaying it to an external receptor. Each input parameter will have respective weight factors and activation functions. The error is then calculated using the method of mean squared error and is propagated back through the network to update the weights and reduce the error. Fig. 2 demonstrates the logic behind it [Pal 2015].

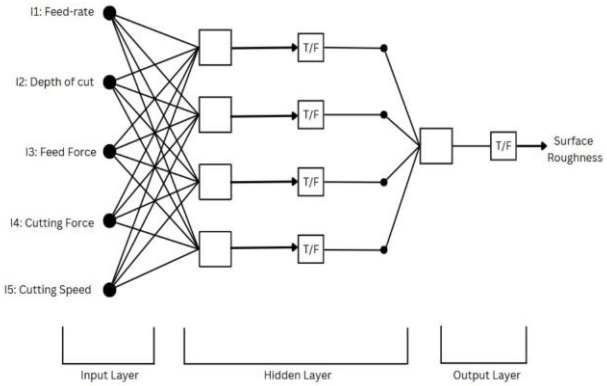

Fig. 2: ANN Architecture Example

2.3 CNN

CNNs belong to the class of deep learning algorithms. They are known for their ability to adaptively learn spatial features or hierarchies from the input image and classify this image according to its dominant features. The main layers are introduced:

Convolutional Layers: A kernel of changeable weights convoluted over the image performing an element-by-

element matrix multiplication between the filter and pixels. After summing up the obtained values for each feature, the number will be stored in a feature map. High values will indicate that a feature is prominent, while lower values deem the feature as absent or dim.

Rectified Linear Unit (ReLU): This activation function sets all negative values in the feature map to zero, introducing non-linearity that helps the network learn complex patterns more effectively.

Pooling Layer: This layer downscales the feature map and retains the prominent features. It is used to reduce computational complexity, retain important features, and prevent overfitting.

Softmax Layer: Probabilities of the different categories are distributed to the input image. The feature with the highest probability will be the classifying parameter [Cong 2023].

The CNN used for training is the deep convolutional neural network known as GoogleNet, which was first released by Google in 2014. It is known for its inception module, which combines convolutional layers with varying kernel sizes (1x1, 3x3, 5x5) and pooling layers in parallel. It processes features at numerous scales. With 22 layers, GoogleNet is computationally efficient because of 1x1 convolutions, which optimize performance while lowering parameters. GoogleNet has proved to be more accurate (with an accuracy of 0.95 for grayscale and 0.96 for RGB) than both AlexNet and custom CNNs [Szegedy 2015].

3 EXPERIMENTATION

The experimentation phase involves simulations related to UVAT

To operate the piezoelectric material, a signal generator and a high-voltage power amplifier were employed. An HDG3000B-series arbitrary waveform generator, capable of supporting frequencies from 1 μHz to 100 MHz, provided the input signal. This voltage was then amplified by a PZD350A high-voltage amplifier, which can deliver up to 350 V. An exponential ultrasonic concentrator, made from Aluminum 6061, was designed to increase the amplitude of vibration, ensuring a significant effect on the workpiece. Using this setup, micro-scale dimples were successfully generated. This outcome was achieved through precise tuning and control of key parameters, including cutting speed, feed rate, depth of cut, frequency, and amplitude.

Ongoing work is underway to optimize the dimples' geometry; however, Fig. 3 shows preliminary results obtained by passing a metal sheet across a tool resonating at 17kHz with a 488 ohms resistance.

Fig. 3: Experimental Micro-Textures

While the experimental results are still being optimized, AI codes were developed for theoretical calculations and theoretical shapes. Future work will include re-training the AI with experimental data and images to calculate the similarity ratio and repeatability across the workpiece.

The experiments will be divided into two types of analyses, as demonstrated in Fig. 4. First, the kinematic relations that relate to the machining parameters and dimples geometry for UVAT will be used with ANN for process optimization and parametric micro-texture analysis. The next step is to simulate dimples and classify them based on their shapes and edges by using CNN.

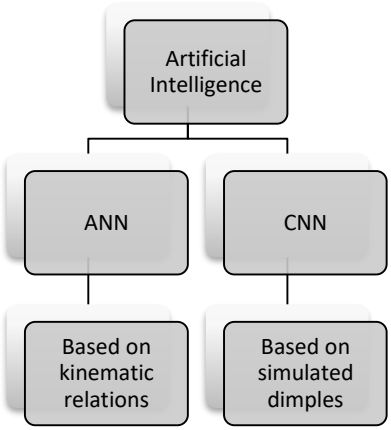

Fig. 4: AI DOE

3.1 ANN

To find the relation that would generate accurate predictions and classification for unseen data, ANN will be fed with both inputs and outputs. The inputs include the speed, frequency, workpiece radius, nose radius, feed and amplitude. As for the outputs, they consist of the dimples' length and width. To teach the AI these relations, both inputs and outputs will be based on literature review and dimples geometry calculated from the kinematic equations expressed in the literature review.

Tab.1 was prepared, containing both inputs and outputs.

Tab. 1: ANN Sample Input and Output

Inputs							Outputs	
Speed (mm/sec)	**Frequency (Hz)**	**Workpiece Radius (mm)**	**Nose Radius (mm)**	**Feed (mm)**	**Amplitude (microns)**	**K (number of dimples along one circumferential surface of the workpiece)**	**Width (mm)**	**Length (mm)**
1666.67	24000.00	11.50	0.25	0.10	2.20	864.00	0.09	0.07
2000.00	24000.00	11.50	0.25	0.10	2.20	720.00	0.09	0.08
2500.00	24000.00	11.50	0.25	0.10	2.20	576.00	0.09	0.10
3000.00	24000.00	11.50	0.25	0.10	2.20	480.00	0.09	0.13
3500.00	24000.00	11.50	0.25	0.10	2.20	411.43	0.09	0.15
4000.00	24000.00	11.50	0.25	0.10	2.20	360.00	0.09	0.17

The inputs followed the one-variable-at-a-time method, in which one input is changed each round to observe how the change of each parameter affects the outcome. The selected input parameters and their conditions were: feed (kept greater than the dimple width to prevent overlap), speed (varied between 100 and 1000 m/min), and dimple alignment (maintained without phase shift). Table 1 summarizes six representative rounds out of a total of 97 experimental runs.

The table is then fed to MATLAB to be used in the "Neural Net Fitting." The number of hidden layers was chosen to be 7 by cross-validation, a statistical technique used to evaluate the model by testing the model with unseen data to reduce overfitting. Converging results were obtained for the following ANN architecture in Fig. 5.

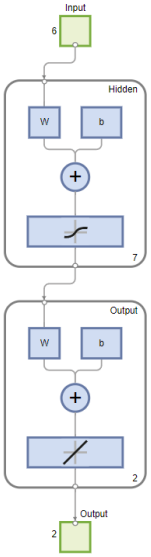

Fig. 5: ANN Architecture

The training algorithm that was used is Levenberg-Marquardt (LM), a well-established second-order optimization technique for training feedforward neural networks. It functions by minimizing the sum of squared error between the network's predicted output and target values. Its key advantages are its fast convergence, robustness to initial parameter estimations, and ability to handle non-linear relations [Okkan 2011].

After several training iterations, Fig 6 shows the training results where the line of best fit is achieved:

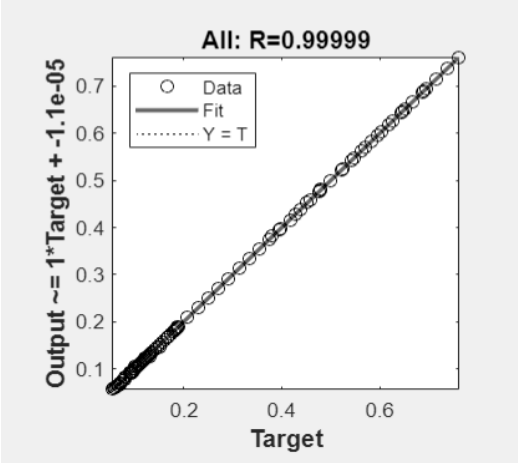

Fig. 6: ANN Training Results

The regression plot shows a strong agreement between the ANN predictions and target values across training, validation, and testing datasets. The overall regression coefficient is R=0.9999, confirming that the network accurately captured the input-output relationship. Indeed, the regression line nearly overlaps with the trendline Y=T.

Fig. 7 shows the mean squared error and its performance plot.

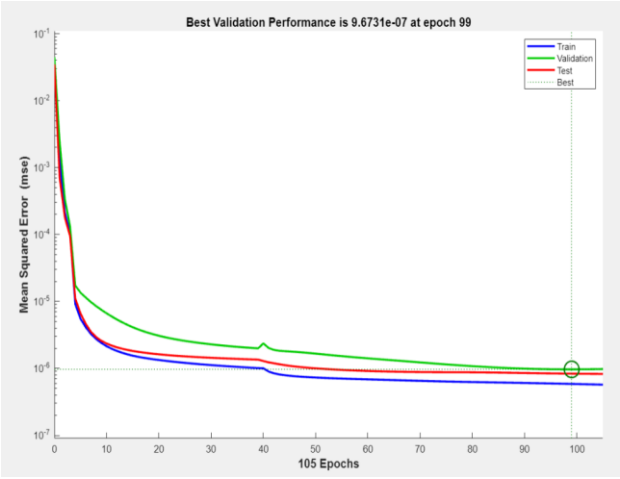

Fig. 7: ANN Mean Squared Error

The mean squared error graph demonstrates how the ANN successfully captured the underlying relationship between the input parameters and the resulting micro-texture dimensions. The training, validation, and test errors decreased consistently over the epochs, indicating that the model was effectively learning without large fluctuations. Importantly, the curves remained close to each other, which points to good regularization and strong generalization of the model. The plateau towards the end suggests the onset of minor overfitting, but this effect is limited because the overall network was robust and converged at an optimal point where validation error reached its minimum. And so, the ANN was able to converge with an error of 10^{-6}.

The regression curves for the predicted dimple width and length are shown in Fig. 8 and 9, respectively. For the width, the maximum deviation from the actual values was 4.72%, while for the length, the maximum deviation was 2.68%. These small deviations indicate that the trained artificial neural network accurately captured the underlying relationship between the input features and the output dimensions, demonstrating the validity and reliability of the model.

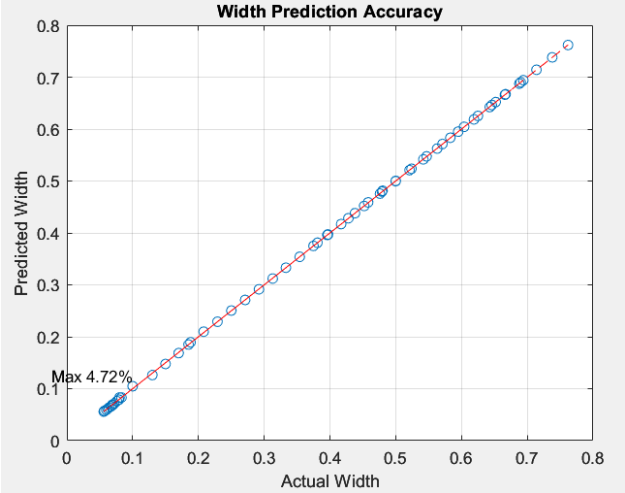

Fig. 8: Width Prediction Accuracy

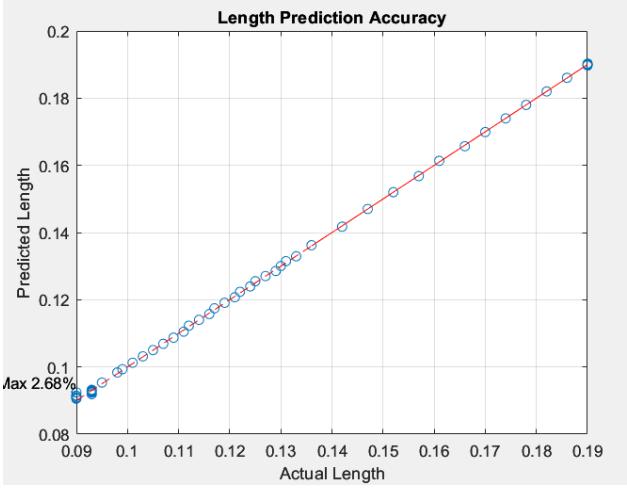

Fig. 9: Length Prediction Accuracy

For future work, the training will be repeated using experimental results to compare the calculated and actual dimple sizes. The deviation will be due to BUE, thermal-induced effects, chip quality, and other factors that are not accounted for in theoretical calculations.

3.2 CNN

Using a pre-trained network on MATLAB, the performance of GoogleNet will be evaluated, specifically in categorizing and identifying simulated dimples that will be imprinted micro-features in manufacturing companies.

The micro-scale dimples are simulated: some have oval shapes (reflecting the true geometry of the dimples), and others are defective (which occurs during machining) as seen in Fig. 10.

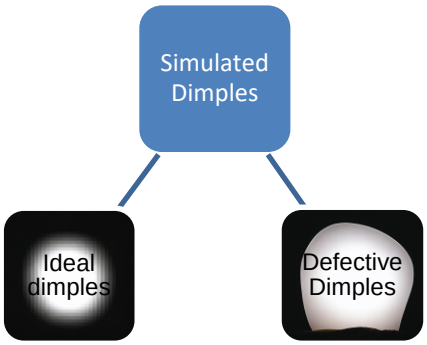

Fig. 10: Simulated Dimples' Shapes: Round vs. Irregular shape.

The oval shaped dimples, considered as the ideal ones, are produced by carefully controlling the electrical and machining parameters to achieve round shapes that are both repeatable and reproducible. These dimples exhibit symmetry and uniformity, with consistent geometry replicated across the entire workpiece. As for the defective ones, they arise from factors such as inconsistencies in the tool nose radius, tool misalignment, inadequate or excessive cutting depth that diminishes the effect of vibrations, as well as inappropriate vibration frequencies or amplitudes. Such conditions lead to irregular, asymmetric shapes and a lack of uniformity in the textured surface.

These textures were simulated using a drawing software to generate synthetic images, on which gradient-based attribution methods were applied to realistically represent textured shapes.

The training is divided into three stages: first, there is an input dataset that will be trained. Second, the input set will be compared to a validation dataset for training. Third, to make sure that the validation accuracy truly reflects the model's generalization ability and is not overly dependent on the validation dataset, a testing dataset will be used to find the precision and recall after training. Precision and recall are key performance metrics that can be derived from a confusion matrix, which summarizes the classification results into four categories consisting of: true positives (TP), false positives (FP), true negatives (TN), and false negatives (FN). They can be derived from the following equations:

$$Precision = \frac{TP}{(TP+FP)} \quad (6)$$

$$Recall = \frac{TP}{(TP+FN)} \quad (7)$$

Precision measures the percentage of correctly predicted positive samples out of all the samples the model predicted as positive, indicating its effectiveness in minimizing false positives. Recall measures the percentage of correctly predicted positive samples out of all the samples that are positive in reality, reflecting the model's ability to identify all true positives. Together, these metrics provide

complementary perspective on the classification performance of the trained dataset [Valizadeh 2022].

The input dataset for each category contained 100 images. Ten percent of these images were reserved for testing after training, leaving 90 images for model development. Of these 90 images, approximately 15% (13 images) were allocated for validation during training, and the remainder were used for the training process. To enhance dataset diversity and improve the robustness of the model, image augmentation was performed in MATLAB. The augmentation process included rotations at two distinct angles, translations, scaling to multiple sizes, and shearing transformations. These operations increased the training dataset from 90 to 540 images and the testing dataset from 10 to 60 images, thereby improving the model's ability to generalize to unseen data.

During training, the choice of solver significantly influences the model's accuracy and validation performance. In this study, the selected solver was Stochastic Gradient Descent with Momentum (SGDM), a widely adopted optimization method in deep learning. SGDM updates the model's parameters iteratively based on the gradient of the loss function computed from a mini batch of training data, rather than the entire dataset. This approach enables faster computation and more efficient convergence while maintaining stability compared to standard gradient descent [Wang 2017]. Second, the Initial Learning Rate depicts the rate at which the model changes after each iteration based on the estimated error and the assigned weights that will be updated as well. As for the validation frequency, it refers to the number of times the training is compared to the validation set. Finally, the mini-batch size refers to the number of images used in one iteration.

The results of the training are tabulated in Tab. 2.

Among the tested configurations, the second input values (learning rate of 0.0001, mini batch size of 4, and validation frequency of 5) achieved the highest validation accuracy of 96.15%, along with precision and recall values of 0.92 and 0.93, respectively. This setup outperformed the third configuration (learning rate of 0.001, mini batch size of 4), which reached only 87.5% validation accuracy, highlighting that a lower learning rate allowed the network to converge more stably. Furthermore, the use of a smaller mini batch size (4 compared to 8 in the first setup) led to more frequent gradient updates, which improved generalization and resulted in higher accuracy compared to the first configuration (92.31%).

The training progress shown in Fig. 11 confirms this behavior. The training accuracy, demonstrated by the solid blue line, increases rapidly and stabilizes above 95%, while the validation accuracy, demonstrated by the dashed black line, follows closely, consistently staying above 90%. The proximity between the training and validation curves demonstrates the robustness of the model and suggests that overfitting did not occur. Although minor fluctuations are observed in the initial epochs, the model stabilizes during later epochs, which validates the effectiveness of the chosen parameters.

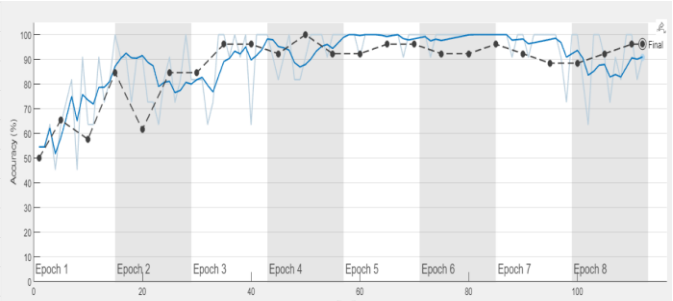

Fig. 11: GoogleNet Training Validation Accuracy

GoogleNet was able to successfully classify micro-textures with high accuracy, demonstrating its potential for use in industrial settings. The successful classification of these dimples provides direct evidence that CNNs can be reliably used as a quality control tool in industrial applications, where consistent monitoring of micro-features is critical.

4 CONCLUSION

While previous studies in literature have investigated UVAT as a process and others have separately applied neural networks for image recognition and classification tasks, the two approaches have not been combined. The present work addresses this gap by establishing the feasibility of AI-driven neural networks (ANN and CNN) in micro-texture analysis and classification. ANN was able to find the underlying relationship between the machining parameters and dimple shape. It will thus enable the prediction of the required process parameters to obtain specific dimple dimensions. Future work will encompass fine-tuning the networks to account for real-time alterations in machining that will optimize the resulting shape. As for CNN, it was able to accurately categorize the dimples and defective shapes. It serves as a quality assurance tool that evaluates the produced textures and can give similarity ratios and tolerance checks of the workpiece to ensure meeting industrial standards. This work will thus be focused on evaluating different CNN architectures, inputting real-world machining images, and integrating the defect classification in real-time for the UVAT manufacturing process.

Tab. 2: CNN Input and Output Parameters

	Input				Output		
Network	**Initial Learning Rate**	**Validation Frequency**	**Max Epochs**	**Mini Batch Size**	**Validation Accuracy**	**Precision**	**Recall**
GoogleNet	0.0001	5	8	8	92.31%	0.9	0.904
	0.0001			4	96.15%	0.92	0.93
	0.001			4	87.50%	0.85	0.865

5 REFERENCES

[Akkus 2011] Akkus, H. and Asiltruk, I. Predicting Surface Roughness of AISI 4140 Steel in Hard Turning Process through Artificial Neural Network, Fuzzy Logic, and Regression Models. Scientific Research and Essays, July 2011, Vol. 6, No. 13., pp 2729-2736. ISSN 1992-2248.

[Cong 2023] Cong, S. and Zhou, Y. A Review of Convolutional Neural Network Architectures and their Optimizations. Artificial Intelligence Review, March 2023, Vol. 56, No. 3., pp 1905-1969. ISSN 0269-2821.

[Heidari 2015] Heidari, F. Micromachining: A New Trend in Manufacturing. In: 120th ASEE Annual Conference & Exposition, Texas A&M University, Kingsville, June 2013, pp 9071-9077.

[Krishnamoorthy 2004] Krishnamoorthy, K., Lin, C.Y., and Tsao, T.C. Design and Control of a Dual-Stage Fast Tool Servo for Precision Machining. In: Proceedings of the 2004 IEEE International Conference on Control Applications, Taipei, Taiwan, September 2004, pp. 742-747.

[Lengerov 2023] Lengerov, A.L., Sabey, S., and Paliiski, S. Experimental Study of Surface Roughness in Vibro-Impact Cutting of Optical Slugs. In: Environment. Technology. Resources. Proceedings of the International Scientific and Practical Conference, Rezekne, Latvia, June 2023, pp. 145-148.

[Liu 2018] Liu, X., Wu, D., Zhang, J., Hu, X., and Cui, P. Analysis of Surface Texturing in Radial Ultrasonic Vibration-Assisted Turning. Journal of Materials Processing Technology, December 2018, Vol. 267, pp. 186-195. ISSN 0924-0136.

[Liu 2019] Liu, X., Wu, D., Zhang, J., Hu, X., and Cui, P. Influence of Tool Material and Geometry on Micro-Textured Surface in Radial Ultrasonic Vibration-Assisted Turning. International Journal of Mechanical Sciences, March 2019, Vol. 152, pp. 545-557. ISSN 0020-7403.

[Nestler 2014] Nestler, A. and Schubert, A. Surface Properties in Ultrasonic Vibration Assisted Turning of Particle Reinforced Aluminum Matrix Composites. Procedia CIRP, December 2014, Vol. 13, pp 125-130. ISSN 2212-8271.

[Okkan 2011] Okkan, U. Application of Levenberg-Marquardt Optimization Algorithm Based Multilayer Neural Network for Hydrological Time Series Modeling. An International Journal of Optimization and Control: Theories and Applications, June 2011, Vol. 1, No. 1., pp 53-63. ISSN 2146-0957.

[Osterrieder 2020] Osterrieder, P., Budde, L., and Friedli, T. The Smart Factory as a Key Construct of Industry 4.0: A Systematic Literature Review. International Journal of Production Economics, March 2020, Vol. 221. ISSN 0925-5273.

[Pal 2005] Pal, S.K. and Chakraborty, D. Surface Roughness Prediction in Turing Using Artificial Neural Network. Neural Computing and Applications, June 2005, Vol. 14, No. 4., pp. 319-324. ISSN 1433-3058.

[Schubert 2011] Schubert, A., Nestler, A., Pinternagel, S., and Zeidler, H. Influence of Ultrasonic Vibration Assistance on the Surface Integrity in Turning of Aluminum Alloy AA2017. Materials Science & Engineering Technology, July 2011, Vol. 42, No. 7., pp. 658-665.

[Sharma 2016] Sharma, V. and Pandey, P.M. Recent Advances in Ultrasonic Assisted Turning: A Step towards Sustainability. Cogent Engineering, May 2016, Vol. 3, No. 1., pp 1-20.

[Szegedy 2015] Szegedy, C., Liu, W., Jia, Y., Sermanet, P., Reed, S., and Anguelov, D. Going Deeper with Convolutions. In: 2015 IEEE Conference on Computer Vision and Pattern Recognition, Boston, USA, June 2015, pp 1-9. ISBN 1063-6919.

[Valizadeh 2022] Valizadeh, M. and Wolff, S.J. Convolutional Neural Network Applications in Additive Manufacturing: A Review. Advances in Industrial and Manufacturing Engineering, May 2022, Vol. 4, pp 100072. ISSN 2666-9129

[Wang 2022] Wang, J., Bai, X., Shen, X., Liu, X., and Wang, B. Effect of Micro-Texture on Substrate Surface on Adhesion Performance of Electroless Ni-P Coating. Journal of Manufacturing Processes, February 2022, Vol. 74, pp 296-307. ISSN 1526-6125.

[Wang 2017] Wang, T., Chen, Y., and Qiao, M. A Fast and Robust Convolutional Neural Network-Based Defect Detection Model in Product Quality Control. International Journal of Advanced Manufacturing Technology, August 2017, Vol. 94, No. 9., pp 3465-3471. ISSN 1433-3015.

[Zhong 2006] Zhong, Z., Khoo, L.P., and Han, S.T. Prediction of Surface Roughness of Turned Surfaces using Neural Networks. International Journal of Advanced Manufacturing and Technology, April 2006, Vol. 28, No. 7., pp 688-693. ISSN 1433-3015.